



Research paper

Crystal structure of Bn IV in complex with myristic acid: A Lys49 myotoxic phospholipase A₂ from *Bothrops neuwiedi* venom

P. Delatorre^{b,**}, B.A.M. Rocha^a, T. Santi-Gadelha^b, C.A.A. Gadelha^b, M.H. Toyama^c, B.S. Cavada^{a,*}

^a Departamento de Bioquímica e Biologia Molecular, Universidade Federal do Ceará, P. O. Box: 6043, Zip Code: 60.455-970, Fortaleza, Brazil

^b Departamento de Biologia Molecular, Universidade Federal da Paraíba, Zip Code: 58059-900, João Pessoa, Paraíba, Brazil

^c Universidade Estadual Paulista-UNESP, Campus do Litoral Paulista–Unidade São Vicente, Brazil

ARTICLE INFO

Article history:

Received 26 August 2010

Accepted 16 November 2010

Available online 22 November 2010

Keywords:

Phospholipase A₂

Myristic acid

Myotoxin

Heparin

ABSTRACT

The LYS49-PLA₂s myotoxins have attracted attention as models for the induction of myonecrosis by a catalytically independent mechanism of action. Structural studies and biological activities have demonstrated that the myotoxic activity of LYS49-PLA₂ is independent of the catalytic activity site. The myotoxic effect is conventionally thought to be due to the C-terminal region 111–121, which plays an effective role in membrane damage. In the present study, Bn IV LYS49-PLA₂ was isolated from *Bothrops neuwiedi* snake venom in complex with myristic acid (CH₃(CH₂)₁₂COOH) and its overall structure was refined at 2.2 Å resolution. The Bn IV crystals belong to monoclinic space group P2₁ and contain a dimer in the asymmetric unit. The unit cell parameters are $a = 38.8$, $b = 70.4$, $c = 44.0$ Å. The biological assembly is a “conventional dimer” and the results confirm that dimer formation is not relevant to the myotoxic activity. Electron density map analysis of the Bn IV structure shows clearly the presence of myristic acid in catalytic site. The relevant structural features for myotoxic activity are located in the C-terminal region and the Bn IV C-terminal residues NKKYRY are a probable heparin binding domain. These findings indicate that the mechanism of interaction between Bn IV and muscle cell membranes is through some kind of cell signal transduction mediated by heparin complexes.

© 2010 Elsevier Masson SAS. All rights reserved.

1. Introduction

Phospholipases A₂ (PLA₂–EC 3.1.1.4, phosphatide sn-2 acylhydrolase) are stable calcium-dependent enzymes. They are membrane-associated proteins and their importance is related to catalysis of membrane phospholipids. PLA₂ hydrolyzes the second ester bond of 1,2-diacyl-3-phosphoglycerides to liberate free fatty acids and lysophospholipids [1]. Certain biological activities attributed to PLA₂s have been previously reported, including neurotoxic, myotoxic, anticoagulant, hypotensive, cardiotoxic, edema-inducing and bactericidal. [2,3,4,5,6].

Myotoxins are defined as proteins/peptides components of venom secretions that induce irreversible damage to skeletal muscle fibers (myonecrosis) upon injection into animals. Some myotoxins act locally, damaging muscle fibers at the site of

injection and its surroundings, whereas others act systemically, causing muscle damage at distant sites [7].

The phospholipase A₂ myotoxins can be divided into two groups: neurotoxic and non-neurotoxic. Non-neurotoxic myotoxins can be classified in two different types based on the amino acid residue 49: ASP49-PLA₂, which catalyzes the hydrolysis of ester bond at sn-2 position of glycerophospholipids, and LYS49-PLA₂ (or PLA₂-like proteins), which are characterized by the absence of enzymatic activity. Irrespective of their ability to catalyze phospholipid hydrolysis (ASP49-type) or not (LYS49-type), all of the non-neurotoxic PLA₂s myotoxins, as implied by their name, induce skeletal muscle damage. Thus, the LYS49-PLA₂ myotoxins have attracted attention as models for the induction of myonecrosis by a catalytically independent mechanism of action.

Structural studies and biological activities have demonstrated that the myotoxic activity of LYS49-PLA₂ is independent of the catalytic activity site, but related to the C-terminal domain, KKYR-YYLKPLCKK. Peptides made from this short segment showed myonecrotic and cytolytic activities and bactericidal effects [7].

The LYS49-PLA₂s have been described as inactive enzymes against most substrates commonly tested for PLA₂s, such as lecithin from egg yolk phospholipids and other isolates. A possible explanation for the

* Corresponding author. Tel./fax: +55 85 40089818.

** Corresponding author.

E-mail addresses: pldelatorre@gmail.com (P. Delatorre), bscavada@ufc.br (B.S. Cavada).

low catalytic activity of LYS49-PLA₂s has been suggested by Lee and co-workers [8], who noted fatty acid bound in the catalytic sites of certain enzymes. These authors proposed a mechanism by which LYS49-PLA₂ would promote the hydrolysis of certain phospholipids, especially those negatively charged. Thus the free fatty acid produced in the reaction would not move from the active center, inhibiting the enzymes for subsequent reactions. An alternative mechanism which refutes the previous hypothesis is that catalytic activity is absent because calcium is not bound to the calcium binding site due to steric interference from the lysine side chain [9].

This work describes the crystal structure of a LYS49-PLA₂, isolated from the venom of *Bothrops neuwiedi* (Bn IV), in complex with myristic acid (CH₃(CH₂)₁₂COOH), and indicates the possible existence of a heparin binding site in the Bn IV C-terminal region.

2. Materials and methods

2.1. Crystallization and X-ray data collection

The myotoxins from *Bothrops neuwiedi* snake venoms were characterized biochemically by Rodrigues and co-workers [10]. The Bn IV was purified using a two-step chromatographic procedure according to the methods described by Toyama and co-workers [11]. Firstly, 10 mg of the crude venom was dissolved in 250 μ L loading buffer (0.05 M Tris–HCl, pH 8.0) and centrifuged at 4500 \times g for 5 min. The supernatant was loaded onto a BioSuite Q anion exchange column (Waters.Co). Proteins were eluted from the column gradient with a buffer containing 0.05 M Tris–HCl, pH 8.0, with increasing concentrations of 1.0 M NaCl at a constant flow rate of 1 mL/min. The Bn IV myotoxic fractions obtained in the first chromatographic step were dissolved in 250 μ L of an aqueous solution containing 0.15% trifluoroacetic acid and loaded onto an X-Terra C18 analytical reverse phase column. Proteins were eluted using a mobile phase of 0.15% aqueous trifluoroacetic acid (TFA) with increasing quantities of 66% acetonitrile at a constant flow rate of 1 mL/min [12].

The purified Bn IV was lyophilized and dissolved at a concentration of 10 mg mL⁻¹ in 1 mM Tris–HCl pH 7.4 for use in crystallization trials. Small crystals grew in 0.1 M Tris–HCl pH 8.5, 0.2 M lithium sulfate containing 30% (w/v) PEG 4000, using the hanging-drop vapor-diffusion method in Linbro plates at 293 K. The drops were composed of equal volumes (2 μ L) of protein solution and reservoir solution and were equilibrated against 300 μ L reservoir solution. The initial condition was optimized and best crystals were obtained in 0.1 M Tris–HCl pH 8.5 containing 20% (w/v) PEG 4000 (Sigma–Aldrich, St.Louis, MO, USA). The X-ray diffraction data were collected at 1.42 Å wavelength at beamline MX1 station (Laboratório Nacional de Luz Síncrotron–LNLS, Campinas, Brazil) using a CCD (MAR research) imaging plate at 105 mm crystal to detector distance. A set of 180 images (1° oscillation) was recorded. Diffraction data were indexed, integrated and scaled using MOSFLM [13] and SCALA [14].

2.2. Protein structure determination

The Bn IV structure was solved by molecular replacement with the program MOLREP [15], using the monomer structure of the native LYS49-PLA₂ from *Bothrops neuwiedi pauloensis* [PDB code 1PC9] as search model [16]. Crystallographic refinement was carried out by cycles of maximum likelihood refinement with the program Refmac 5 [17].

Initially, a simple rigid body refinement was run to verify the relative position of Bn IV rigid groups. Next, a restrained refinement was performed with correction and substitution of amino acid side chains, using the Fo-Fc electron density map generated and visualized by WinCoot [18]. Water molecules were added by WinCoot

and inspection was carried by Fourier difference maps and stereochemical criteria. An anisotropic restrained refinement was also performed and the quality of the Bn IV model was checked using the Procheck program [19]. Visualization was carried out by WinCoot and Pymol [20]. An omit map contoured at 3 σ to fatty acid was generated using the CCP4 Omit program [18].

2.3. Ligand binding site prediction

Two strategies were followed to predict ligand sites. Q-SiteFinder [21], a ligand binding site prediction program, based on determining energetically favorable binding sites on the surface of a protein, can determine if sites have volumes roughly equivalent to ligand volumes irrespective of the overall size of the protein. Molegro Virtual Docker [22], is an integrated platform for predicting protein–ligand interactions, The built-in cavity detector identifies promising binding locations.

3. Results and discussion

3.1. Protein sequencing analysis

The Bn IV sequence is a polypeptide chain composed of 121 amino acid residues with a molecular mass of 14 kDa. The Bn IV sequence is highly similar to other myotoxic PLA₂s. The best alignment scores using Blast were with PLA₂s from *Bothrops neuwiedi*, fraction-6 and 7, and PRTX-I, representing 99, 98% and 97.5%, respectively. The best result for ASP49-PLA₂ was for *Bothrops jararacussu* PLA₂ with 52% similarity, confirming the myotoxic properties. The sequence alignment of the Bn IV with other PLA₂s shows that the third alpha helix is highly conserved, with the exception of only one residue compared to other species (Fig. 1). The first alpha helix is conserved only in LYS49-PLA₂ and the N-terminus, which runs to residue 15, is strongly implicated in the role of toxicity in LYS49-PLA₂ [23], although, only LYS7 residue is responsible for that function [24]. In the Bn IV sequence, only the residue ILE54 is different when compared with other PLA₂s.

3.2. Overall structure

The Bn IV crystal belongs to space group P2₁ with unit cell dimensions of $a = 38.8$, $b = 70.4$, $c = 44.0$ Å and contains a dimer in the asymmetric unit. The structure refinement converges to R_{factor} value 0.202 and R_{free} 0.236. The final model present high stereochemical quality and Ramachandran plot analysis does not show residues in disallowed regions (Table 1).

The Bn IV crystal structure has a conventional dimer oligomerization (Fig. 2). The secondary structure of Bn IV presents mainly alpha-helices with an up-down bundle architecture and phospholipase A2 topology, being composed of an N-terminal alpha helix, a calcium binding loop, two anti-parallel alpha helices, two short anti-parallel beta sheet (β -wings), and a C-terminal loop.

The calcium binding site is conserved in PLA₂s structures. However, De Azevedo and co-workers [25] observed that the nitrogen (NZ) of the residue LYS49 occupies the calcium site interacting through hydrogen bonding, which blocks Ca⁺² binding and catalytic action (Fig. 3). This action does not inhibit the myotoxic effect, and evidences that myotoxicity occurs even without catalytic activity [8]. The atomic coordinates for Bn IV complexed crystal structure have been deposited in the Protein Data Bank, code 3MLM.

3.3. Fatty acid binding site

Our first step was to determine if PEG 4000 was occupying the fatty acid binding site. The electron density map (Fo-Fc) in the

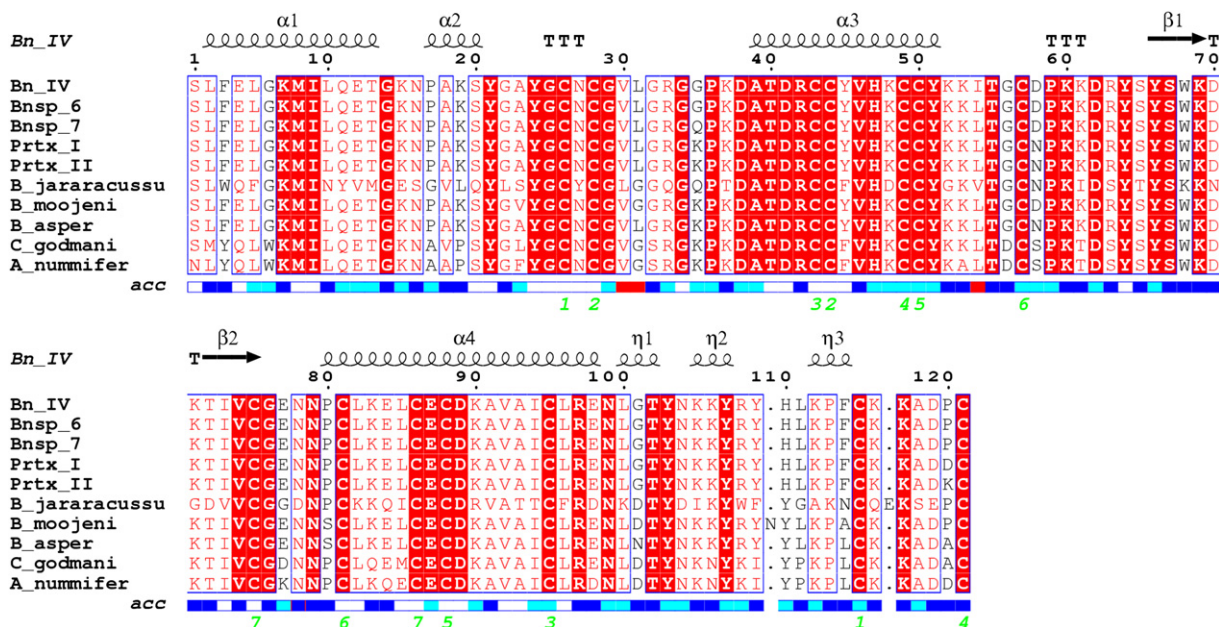


Fig. 1. Bn IV multiple alignment with other PLA₂s. The red boxes show conserved amino acids and colorless boxes show semi-conservative substitutions. Disulfide bridges are numbered in green. (For interpretation of the references to colour in this figure legend, the reader is referred to the web version of this article).

Table 1

Statistical data collection and molecular refinement.

Data Collection	Bn IV
Total reflections	127,445
Number of unique reflections	11,127
R_{merge}^a (%)	9.0 (30.6)
Resolution limits (Å)	41.52–2.20 (2.32–2.20)
Completeness (%)	96.0 (88.6)
Multiplicity	3.4
$I/\sigma(I)$	6.5 (2.3)
Beamline wavelength (Å)	1.421
Space group	$P2_1$
Unit cell parameters (Å)	$a = 38.8$ $b = 70.4$ $c = 44.0$
Refinement	
Resolution range (Å)	41.3–2.2
R_{factor}^b (%)	21.62
R_{free} (%)	22.91
Biological assembly	dimer
Number of water molecules	71
RMS deviations from ideal values	
Bond lengths (Å)	0.023
Bond angles (degrees)	1.961
Temperature factors	
Average B value for whole protein chain (Å ²)	22.8
Average B Values for water molecules (Å ²)	24.1
Ramachandran plot	
Residues in most favoured regions (%)	85.9
Residues in additional allowed regions (%)	13.6
Residues in generously allowed regions (%)	0.5

*Values in parentheses represent the high resolution shell.

$R_{merge}^a = \frac{\sum_{hkl} \sum_i |I(hkl) - \langle I(hkl) \rangle|}{\sum_{hkl} \sum_i I(hkl)}$ where $I(hkl)_i$ is the intensity of i th measurement of the reflection h and $\langle I(hkl) \rangle$ is the mean value of the $I(hkl)_i$ for all I measurements.

$R_{factor}^b = \frac{|F_{obs}| - |F_{calc}|}{|F_{obs}|}$

neighborhood of the Bn IV catalytic site displays a strong (3σ), clear, continuous and elongated electron density which begins within the site and extends away from it. The structural features of the region and length of the electron density show that it is not possible for PEG 4000 to fit in the binding site. Taking into account the length of the electron density map and the potential components of the plasma membrane of eukaryotic cells, we modeled the ligand as myristic acid 14:0 (tetradecanoic acid). This molecule was then placed and refined in this position that led to a nearly perfect fitting. It was positioned on the hydrophobic site, which would normally be catalytic in ASP49-PLA₂s, and the omit map was

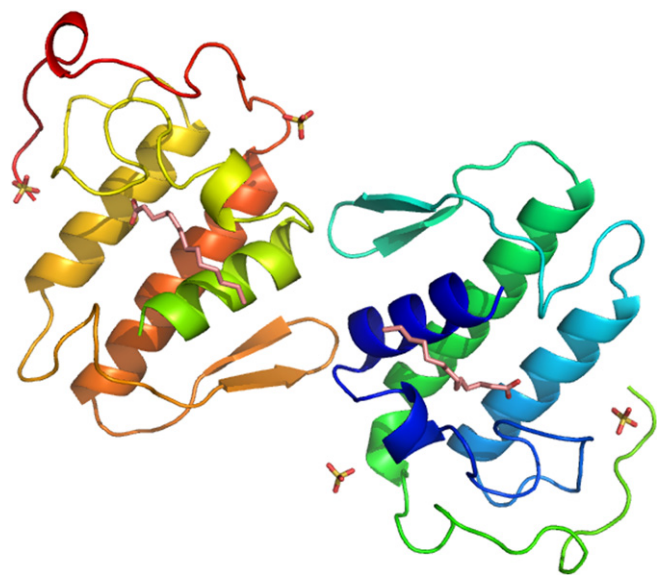


Fig. 2. Overall crystal structure of Bn IV. The dimeric oligomerization forming the conventional dimer with myristic acid (biological interaction) and sulfate ion (crystallization artifact) as ligands.

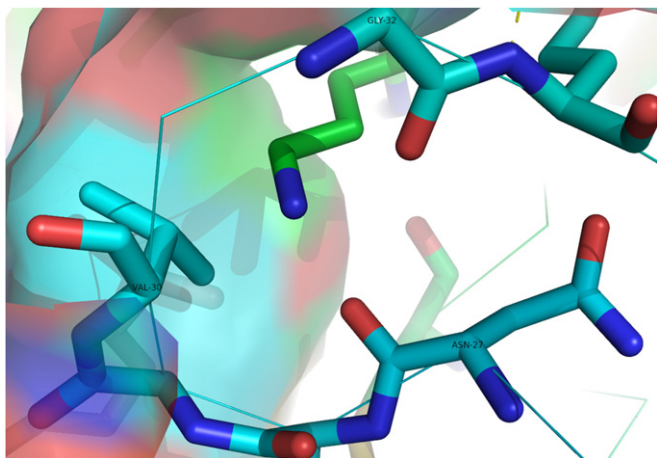


Fig. 3. Calcium binding site occupied by lysine side chain. The nitrogen (NZ) of residue LYS49 of LYS49-PLA₂ occupies the calcium binding site, blocking Ca²⁺ coordination and stopping catalytic action.

generated and confirmed the presence of the ligand (Fig. 4a). The myristic acid is stabilized by hydrogen bonding with ASN27/O2 (2.8 Å), CYS/O (3.0 Å) and HIS47/ND1 (2.4 Å), and also by hydrophobic interactions between the myristic acid and its neighboring

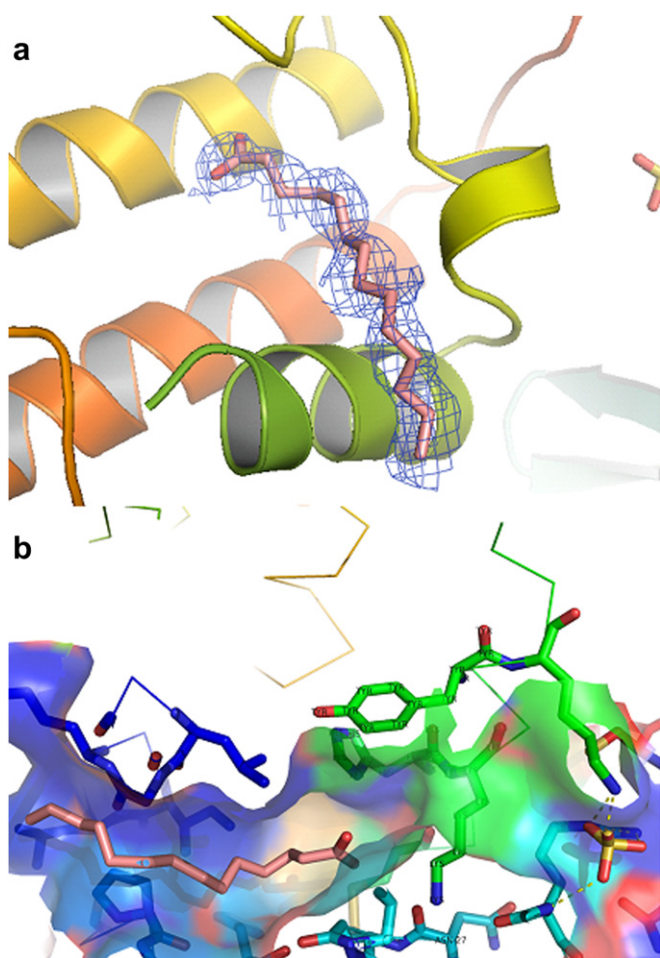


Fig. 4. BN IV fatty acid binding site. (a) Omit map for myristic acid at 2σ and (b) hydrophobic residues interacting with the fatty acid which is placed along the hydrophobic extension which begins within the site and extends away from it.

amino acid residues, LEU2, LEU5, CYS2, TYR21, PRO17, GLY6, LYS7, ALA18, ILE9, LEU111 and PRO113 (Fig. 4b).

The myristic acid interaction with the hydrophobic site in Bn IV and the structural characteristics of this site show that there can be no similarity in function between it and the catalytic site in LYS49-PLA₂s, because local interactions are eminently hydrophobic. This can be confirmed by the existence of many PLA₂s structures interacting with non polar ligands [26,27]. In contrast to this, ASP49-PLA₂s are able to bind Ca²⁺ because they have free calcium binding sites, and this is the determinant to catalysis. Simple mutation of the aspartic acid 49 to lysine makes the side chain of lysine occupy these sites and prevents calcium binding and catalysis. Hydrophobic residues in the region on the inner surface of the N-terminal helix are able to maintain the fatty acid bound to the hydrophobic site without calcium, in contrast to hypothesis proposed by Lee [8] which proposes that the inhibition of LYS49-PLA₂s occurs because the substrate binds tightly resulting in low turnover. So, these myotoxins are incapable of performing catalysis.

3.4. Conventional dimer/alternative dimer

The Bn IV crystal structure, as with all PLA₂s, presents the conventional arrangement stabilized by interactions between the tips of β-wings and the residues of the N-terminal helices [28]. Some authors have proposed the existence of an alternative dimeric conformation that is weakly scientifically supported. The possible alternative arrangement is stabilized by contacts between the putative calcium binding loops and the C-terminus, forming a connection between the active sites of both monomers [29,30]. The former is called the “conventional dimer” since the most of LYS49-PLA₂s structures were solved in this configuration [16]. The latter, “alternative dimer”, is characterized as the configuration with the highest probability of occurring in solution based on the interface area and free energy values calculated by the PISA program [31]. Additionally, recent studies using small angle X-ray scattering experiments [29] and functional aspects were considered to validate alternative dimers.

One face of the monomeric structure of LYS49-PLA₂ has a predominance of hydrophobic amino acid residues (Fig. 5a). The exposure of hydrophobic residues in aqueous solution leads to the formation of closed dimers, which explains the formation of dimers called “alternative” and high free energy values calculated by the PISA program. However, BN IV can also be constructed in alternative dimer form by symmetry operations (−X, Y+1/2, −Z) (Fig. 5b). “Alternative” dimers can be constructed by crystallographic symmetry in all LYS49-PLA₂s represented as conventional dimers, and in small angle X-ray scattering experiments this is equally probable.

The dimer formation is not relevant to the myotoxic activity, since monomers have equal myotoxic activity [32]. Oliveira and co-workers [33] have shown that the dimeric state of the Lys49 myotoxins may contribute to their toxic mechanism in liposomes, since the biological effects were higher at pH 7.2 than at pH 5.0. Ângulo and co-workers [32] showed using cultured myoblasts that the toxic action of LYS49-PLA₂s is not abolished at pH 5.0. Contrasts between liposome and myoblast activities demonstrate that a dimeric state is not an absolute requirement in the muscle-damaging mechanism of LYS49-PLA₂ myotoxins, in monomeric form still being able to exert cell damage.

3.5. Mechanism of action LYS49-PLA₂

The LYS49-PLA₂ mechanism of action is based on the hypothesis that interactions of the molecularly distinct region of the fatty acid

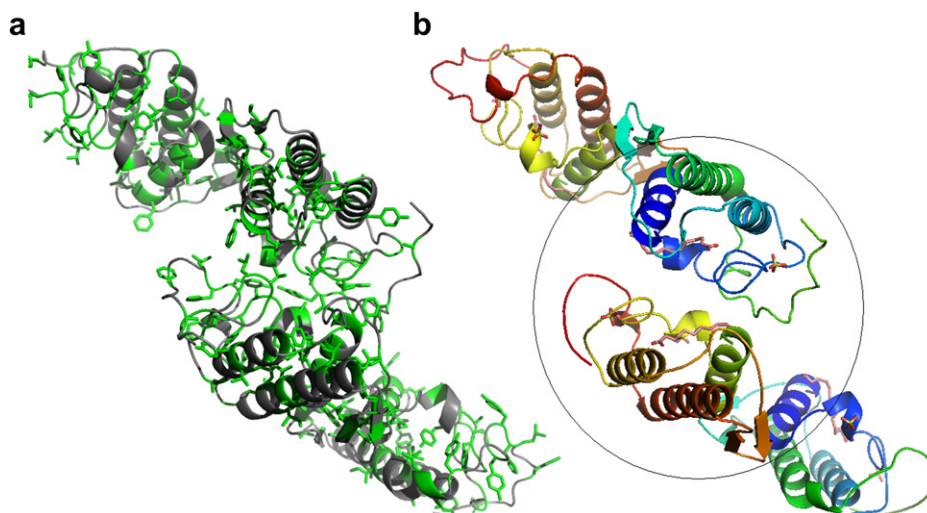


Fig. 5. Alternative dimer assembly of BN IV. (a) View of the interaction between the hydrophobic sides forming the alternative dimer (green). (b) The “alternative” dimer (black circle) can be constructed by crystallographic symmetry of the conventional dimer. Symmetry operator: $-X, Y+1/2, -Z$. (For interpretation of the references to colour in this figure legend, the reader is referred to the web version of this article).

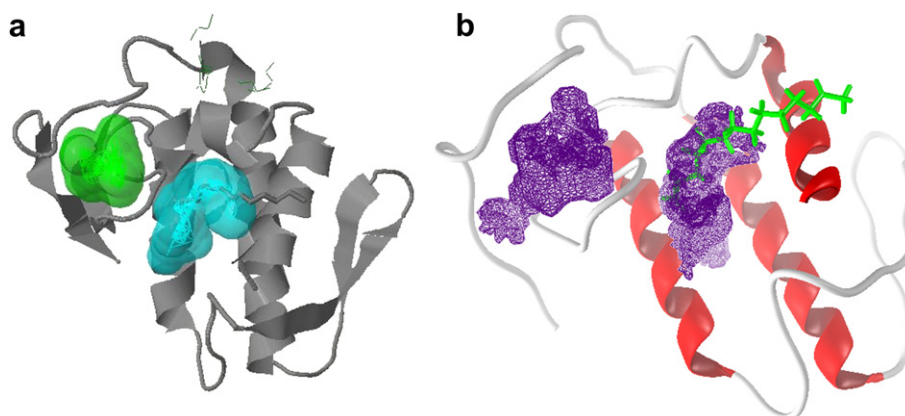


Fig. 6. Prediction of the possible heparin binding site for Bn IV by two different programs: (a) Q-SiteFinder and (b) Molegro Virtual Docker.

binding site with biological membranes are able to destabilize the bilayer.

The myotoxic effect of LYS-PLA₂ has no relationship to its enzymatic activity, since the stereochemical hindrance of the lysine side group blocks the binding of calcium and hence, catalytic activity.

The relevant structural aspects for myotoxic activity are not affected by this change, since apparently the myotoxic activity is related to the C-terminal region of this protein. The myotoxic effect is probably due to the presence of hydrophobic amino acid residues near the C-terminus and the number of basic amino acids present in this region. This allows an electrostatic binding interaction and penetration of the lipid bilayer.

The Bn IV C-terminal residues 104–109 (NKKYRY) are a probable heparin binding domain that facilitates their interaction with heparan sulfate proteoglycans. Heparin binding domains usually follow the consensus sequence for heparin binding proposed by Cardin and Weintraub [34] as follows: XBBBXXBX or XBBXBX, where B is a basic amino acid and X represent non basic amino acids. Moreover, a potential binding pocket (Fig. 6a, b) in the structure of Bn IV was found in the C-terminal region using Molegro Virtual Docker [22] as well as Q-SiteFinder prediction programs [21].

In accordance with this, myotoxic activity of monomeric PLA₂ in experiments conducted at pH 5.0 [28], interactions of PLA₂ with M and N-type membrane receptors [35,36], and with kinase domain receptors [37], inhibition by heparin hexasaccharide [7], neutralization with polyclonal and monoclonal antibodies [38], interaction with cell surfaces via C-terminal heparin binding lysine residues [39] indicate that the mechanisms of myotoxic action must be related to cell signaling, probably by interaction with specific proteoglycans.

4. Conclusion

The strength of interaction between Bn IV and membranes of skeletal muscle cells is not solely related to the existence of positively charged amino acid residues in the C-terminus. These residues interact with negatively charged membrane phospholipids and with hydrophobic/aromatic amino acid residues that are in the monomer positive face and can partially penetrate the membrane. Structurally, low numbers of amino acid residues are probably not able to disrupt membranes. We hypothesize that the high myotoxic activity of Lys49-PLA₂ occurs through some kind of cell signal transduction mediated by heparin complexes. However, this must be confirmed by co-crystallization with heparin.

Acknowledgments

This work was partly financed by Fundação Cearense de Apoio ao Desenvolvimento Científico e Tecnológico (FUNCAP), Conselho Nacional de Desenvolvimento Científico e Tecnológico (CNPq), Coordenação de Aperfeiçoamento de Pessoal de Nível Superior (CAPES), Laboratório Nacional de Luz Síncrotron (LNLS), Campinas—Brazil. BSC, MHT and PD are senior investigators of CNPq. We thank David Erickson for helping with the English language editing of the manuscript.

References

- [1] E.A. Dennis, in: W. Uhl, T.J. Nevalainen, M.W. Buchler (Eds.), *Phospholipase A2: Basic and Clinical Aspects in Inflammatory Diseases*, Karger, Basel, 1997, pp. 307–353.
- [2] S.H. Andrião-Escarso, A.M. Soares, M.R.M. Fontes, A.L. Fuly, F.M. Correa, J.C. Rosa, L.J. Greene, J.R. Giglio, Structural and functional characterization of an acidic platelet aggregation inhibitor and hypotensive phospholipase A2 from *Bothrops jararacussu* snake venom, *Biochem. Pharmacol.* 64 (2002) 723–732.
- [3] S.A. Beers, A.G. Buckland, R.S. Koduri, W. Cho, M.H. Gelb, D.C. Wilton, The antibacterial properties of secreted phospholipases A2. A major physiological role for the group IIA enzyme that depends on the very high pI of the enzyme to allow penetration of the bacterial cell wall, *J. Biol. Chem.* 277 (2002) 1788–1793.
- [4] C.C. Chang, J.D. Lee, D. Eaker, J. Fohlman, Short communications the presynaptic neuromuscular blocking action of taipoxin. A comparison with p-bungarotoxin and crotoxin, *Toxicon* 15 (1977) 571–576.
- [5] R.M. Kini, "Excitement Ahead: structure, function and mechanism of snake venom phospholipase A2 enzymes", *Toxicon* Vol. 42 (2003) 827–840.
- [6] L. Páramo, B. Lomonte, J. Pizarro-Cerdá, J.A. Bengoechea, J.P. Gorvel, E. Moreno, Bactericidal activity of Lys49 and Asp49 myotoxic phospholipases A2 from *Bothrops asper* snake venom: synthetic Lys49 myotoxin II-(115–129)-peptide identifies its bactericidal region, *Eur. J. Biochem.* 253 (1998) 452–461.
- [7] B. Lomonte, Y. Ángulo, L. Calderón, An overview of lysine-49 phospholipase A2 myotoxins from crotalid snake venoms and their structural determinants of myotoxic action, *Toxicon* 42 (2003) 885–901.
- [8] W.H. Lee, M.T. da Silva-Giotto, S. Marangoni, M.H. Toyama, I. Polikarpov, R.C. Garratt, Structural basis for low catalytic activity in Lys49 phospholipases A2 a hypothesis: the crystal structure of piratoxin II complexed to fatty acid, *Biochemistry* 40 (2001) 28–36.
- [9] W.F. de Azevedo Jr., R.J. Ward, F. Canduri, A.M. Soares, J.R. Giglio, R.K. Arni, Crystal structure of piratoxin-I: a calcium-independent, myotoxic phospholipase A2-homologue from *Bothrops pirajai* venom, *Toxicon* 36 (1998) 1395–1406.
- [10] V.M. Rodrigues, A.M. Soares, A.C. Mancin, M. Fontes, M.I. Homs-Brandeburgo, J.R. Giglio, Geographic variations in the composition of myotoxins from *Bothrops neuwiedi* snake venoms: biochemical characterization and biological activity, *Comp. Biochem. Physiol. Part A* 121 (1998) 215–222.
- [11] M.H. Toyama, E.M. Carneiro, S. Marangoni, R.L. Barbosa, G. Corso, A.C. Boschero, Biochemical characterization of two crotonamine isoforms isolated by a single step RP-HPLC from *Crotalus durissus terrificus* (South American rattlesnake) venom and their action on insulin secretion by pancreatic islets, *Biochim. Biophys. Acta.* 1474 (2000) 56–60.
- [12] M.H. Toyama, D.O. Toyama, P.P. Joazeiro, E.M. Carneiro, L.O.S. Beriam, S. Marangoni, A.C. Boschero, Biological and structural characterization of a new PLA(2) from the *Crotalus durissus collilineatus* venom, *Protein J* 24 (2005) 103–112.
- [13] A.G.W. Leslie, Jt. CCP4/ESF–EACBM Newsl. *Protein Crystallogr.* 26 (1992).
- [14] P.R. Evans, Jt. CCP4/ESF–EACBM Newsl. 33 (1997) 22–24.
- [15] A. Vargin, A. Teplyakov, MOLREP: an automated program for molecular replacement, *J. Appl. Cryst.* 30 (1997) 1022–1025.
- [16] A.J. Magro, A.M. Soares, J.R. Giglio, M.R. Fontes, Crystal structures of BnSP-7 and BnSP-6, two Lys49-phospholipases A(2): quaternary structure and inhibition mechanism insights, *Biochem. Biophys. Res. Commun.* 311 (3) (2003) 713–720 Nov 21.
- [17] G.N. Murshodov, A.A. Vagin, A. Lebedev, K.S. Wilson, E.J. Dodson, Efficient anisotropic refinement of macromolecular structures using FFT, *Acta Crystallogr. D55* (1999) 247–255.
- [18] P. Emsley, K. Cowtan, Coot: model-building tools for molecular graphics, *Acta Crystallogr. Sect. D: Biol. Crystallogr.* 60 (12 I) (2004) 2126–2132.
- [19] Collaborative computational program, The CCP4 suite: programs for protein crystallography, *Acta Crystallogr. D50* (1994) 760–763.
- [20] W.L. Delano, The Pymol Molecular Graphics System. DeLano Scientific, San Carlos, CA, 2002.
- [21] A.T.R. Laurie, R.M. Jackson, Q-SiteFinder: an energy-based method for the prediction of protein–ligand binding sites, *Bioinformatics* 21 (9) (2005) 1908–1916.
- [22] R. Thomsen, M.H. Christensen, MolDock: a new technique for high accuracy molecular docking, *J. Med. Chem.* 49 (2006) 3315–3321.
- [23] C. Diaz, A. Alape, B. Lomonte, et al., Cleavage of the NH2-terminal octapeptide of *Bothrops asper* myotoxic lysine-49 phospholipase A2 reduces its membrane-destabilizing effect, *Arch. Biochem. Biophys.* 312 (n.2) (1994) 336–339.
- [24] R.J. Ward, W.F. de Azevedo, R.K. Arni, At the interface: crystal structures of phospholipases A2, *Toxicon* 36 (n.11) (1998) 1623–1633.
- [25] W.F. de Azevedo, R.J. Ward, J.M. Gutiérrez, R.K. Arni, Structure of a Lys49-phospholipase A2 homologue isolated from the venom of *Bothrops nummifer* (jumping viper), *Toxicon* 37 (1999) 371–384.
- [26] C.A.H. Fernandes, D.P. Marchi-Salvadora, G.M. Salvador, Mabel C.O. Silva, T.R. Costa, A.M. Soares, M.R.M. Fontes, Comparison between apo and complexed structures of bothropstoxin-I reveals the role of Lys122 and Ca²⁺-binding loop region for the catalytically inactive Lys49-PLA₂s, *J. Struct. Biol.* 171 (1) (2010) 31–43.
- [27] Q. Liu, Q.Q. Huang, M.K. Teng, C.M. Weeks, C. Jelsch, R.G. Zhang, L.W. Niu, The crystal structure of a novel, inactive, lysine 49 PLA₂ from *Akgistrodon acutus* venom: an ultrahigh resolution, AB initio structure determination, *J. Biol. Chem.* 278 (2003) 41400–41408.
- [28] R.K. Arni, R.J. Ward, J.M. Gutiérrez, A. Tulinsky, Structure of a calcium-independent phospholipase-like myotoxic protein from *Bothrops asper* venom, *Acta Crystallogr.* 51 (1995) 311–317.
- [29] M.T. Murakami, M.M. Viçoti, J.R.B. Abrego, M.R. Lourenzoni, A.C.O. Cintra, E.Z. Arruda, M.A. Tomaz, P.A. Melo, R.K. Arni, Interfacial surface charge and free accessibility to the PLA₂-active site-like region are essential requirements for the activity of Lys49 PLA₂ homologues, *Toxicon* 49 (2007) 378–387.
- [30] J.I. dos Santos, A.M. Soares, M.R. Fontes, Comparative structural studies on Lys49-phospholipases A(2) from *Bothrops* genus reveal their myotoxic site, *J. Struct. Biol.* 167 (2) (2009) 106–116 Aug.
- [31] E. Krissinel, K. Henrick, Inference of macromolecular assemblies from 657 crystalline state, *J. Mol. Biol.* 372 (2007) 774–797.
- [32] Y. Angulo, J. Gutiérrez, A.M. Soares, W. Cho, B. Lomonte, Myotoxic and cytolytic activities of dimeric Lys49 phospholipase A2 homologues are reduced, but not abolished, by a pH-induced dissociation, *Toxicon* 46 (2005) 291–296.
- [33] A.H.C. Oliveira, J.R. Giglio, S.H. Andrião-Escarso, A.S. Ito, R.J. Ward, A pH-induced dissociation of the dimeric form of a lysine 49-phospholipase A2 abolishes Ca²⁺-independent membrane damaging activity, *Biochemistry* 40 (23) (2001) 6912–6920.
- [34] A.D. Cardin, H.J. Weintraub, Molecular modeling of protein–glycosaminoglycan interactions, *Arteriosclerosis* 9 (1989) 21–32.
- [35] J. Nicolas, G. Lambeau, M. Lazdunski, Identification of the binding domain for secretory phospholipases A2 on their M-type 180 kDa membrane receptor, *J. Biol. Chem.* 270 (No. 48) (1995) 28869–28873 Issue of December 1.
- [36] J. Nicolas, Y. Lin, G. Lambeau, F. Ghomashchi, M. Lazdunski, M.H. Gelbi, The Localization of structural elements of bee venom phospholipase A2 involved in N-type receptor binding and neurotoxicity, *J. Biol. Chem.* 272 (Issue 14) (1997) 7173–7181 No. 11.
- [37] Y. Yamazaki, Y. Tokunaga, K. Takani, T. Morita, C-Terminal heparin-binding peptide of snake venom VEGF specifically blocks VEGF-stimulated endothelial cell proliferation, *Pathophysiol. Haemost. Thromb.* 34 (2005) 197–199.
- [38] J.M. Gutiérrez, B. Lomonte, Phospholipase A2 myotoxins from *Bothrops* snake venoms, *Toxicon* 33 (No. 11) (1995) 1405–1424.
- [39] M. Murakami, Y. Nakatani, I. Kudo, Type II secretory phospholipase A2 associated with cell surfaces via C-terminal heparin-binding lysine residues augments stimulus-initiated delayed prostaglandin generation, *J. Biol. Chem.* 271 (47) (1996) 30041–30051 Nov 22.